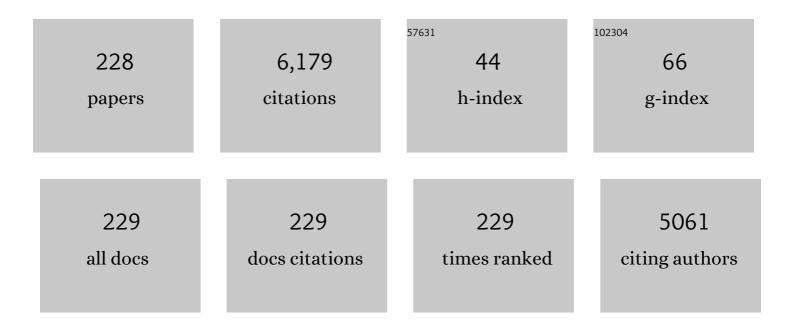
List of Publications by Year in descending order

Source: https://exaly.com/author-pdf/9564474/publications.pdf Version: 2024-02-01



#	Article	IF	CITATIONS
1	Induction heating studies of Fe3O4 magnetic nanoparticles capped with oleic acid and polyethylene glycol for hyperthermia. Journal of Materials Chemistry, 2011, 21, 13388.	6.7	298
2	Verwey Transition in Ultrasmall-Sized Octahedral Fe ₃ O ₄ Nanoparticles. Journal of Physical Chemistry C, 2014, 118, 19356-19362.	1.5	159
3	Sol–gel synthesis, structural and magnetic properties of nanoscale M-type barium hexaferrites BaCoxZrxFe(12â~'2x)O19. Journal of Magnetism and Magnetic Materials, 2014, 350, 23-29.	1.0	157
4	Improved magnetic properties of Cr3+ doped SrFe12O19 synthesized via microwave hydrothermal route. Materials Research Bulletin, 2015, 63, 58-66.	2.7	150
5	Structural, magnetic and dielectric properties of Co-Zr substituted M-type calcium hexagonal ferrite nanoparticles in the presence of α-Fe2O3 phase. Ceramics International, 2018, 44, 17812-17823.	2.3	131
6	Influence of rare earth ion doping (Ce and Dy) on electrical and magnetic properties of cobalt ferrites. Journal of Magnetism and Magnetic Materials, 2018, 449, 319-327.	1.0	130
7	Influence of Co2+ distribution and spin–orbit coupling on the resultant magnetic properties of spinel cobalt ferrite nanocrystals. Journal of Alloys and Compounds, 2013, 566, 54-61.	2.8	123
8	Size dependent magnetic and dielectric properties of nano CoFe2O4 prepared by a salt assisted gel-combustion method. Journal of Applied Physics, 2013, 113, .	1.1	118
9	Cobalt substituted nickel ferrites via Pechini's sol–gel citrate route: X-band electromagnetic characterization. Journal of Magnetism and Magnetic Materials, 2018, 466, 430-445.	1.0	109
10	Structural refinement and photocatalytic activity of Fe-doped anatase TiO2 nanoparticles. Applied Surface Science, 2012, 263, 536-545.	3.1	108
11	Influence of Mg substitution on structural, magnetic and dielectric properties of X-type barium zinc hexaferrites Ba2Zn2-xMgxFe28O46. Journal of Alloys and Compounds, 2018, 741, 377-391.	2.8	100
12	XRD, EDX, FTIR and ESR spectroscopic studies of co-precipitated Mn–substituted Zn–ferrite nanoparticles. Ceramics International, 2019, 45, 8037-8044.	2.3	93
13	Catalytic activities of cobalt, nickel and copper ferrospinels for sulfuric acid decomposition: The high temperature step in the sulfur based thermochemical water splitting cycles. International Journal of Hydrogen Energy, 2011, 36, 4768-4780.	3.8	90
14	Effect of site preferences on structural and magnetic switching properties of CO–Zr doped strontium hexaferrite SrCo x Zr x Fe (12â^'2x) O 19. Journal of Magnetism and Magnetic Materials, 2015, 378, 84-91.	1.0	86
15	Elucidation of phase evolution, microstructural, Mössbauer and magnetic properties of Co2+Al3+ doped M-type Ba Sr hexaferrites synthesized by a ceramic method. Journal of Alloys and Compounds, 2017, 695, 1112-1121.	2.8	86
16	Compositional variability of glauconites within the Upper Cretaceous Karai Shale Formation, Cauvery Basin, India: Implications for evaluation of stratigraphic condensation. Sedimentary Geology, 2016, 331, 12-29.	1.0	82
17	Structural and magnetic characterization of co-precipitated Ni Zn1â^'Fe2O4 ferrite nanoparticles. Journal of Magnetism and Magnetic Materials, 2016, 407, 135-141.	1.0	74
18	Influence of rare earth (Nd+3) doping on structural and magnetic properties of nanocrystalline manganese-zinc ferrite. Materials Chemistry and Physics, 2017, 191, 215-224.	2.0	70

#	Article	IF	CITATIONS
19	Structural and magnetic properties of CuFe2O4 ferrite nanoparticles synthesized by cow urine assisted combustion method. Journal of Magnetism and Magnetic Materials, 2019, 484, 120-125.	1.0	69
20	Synthesis of Low Coercive BaFe12O19 Hexaferrite for Microwave Applications in Low-Temperature Cofired Ceramic. Journal of Electronic Materials, 2013, 42, 761-768.	1.0	65
21	Nanostructured Fe2O3 dispersed on SiO2 as catalyst for high temperature sulfuric acid decomposition—Structural and morphological modifications on catalytic use and relevance of Fe2O3-SiO2 interactions. Applied Catalysis B: Environmental, 2017, 217, 154-168.	10.8	65
22	Preparation and study of magnetic properties of silico phosphate glass and glass-ceramics having iron and zinc oxide. Journal of Magnetism and Magnetic Materials, 2009, 321, 3821-3828.	1.0	63
23	Random site occupancy induced disordered Néel-type collinear spin alignment in heterovalent Zn ²⁺ –Ti ⁴⁺ ion substituted CoFe ₂ O ₄ . RSC Advances, 2015, 5, 91482-91492.	1.7	62
24	Mössbauer, Raman, and Magnetoresistance Study of Aluminum-Based Iron Oxide Thin Films. Journal of Physical Chemistry C, 2011, 115, 3731-3736.	1.5	61
25	Distribution of cations in Co1â^'xMnxFe2O4 using XRD, magnetization and Mössbauer spectroscopy. Journal of Alloys and Compounds, 2015, 646, 550-556.	2.8	61
26	Synthesis of Co-Zr doped nanocrystalline strontium hexaferrites by sol-gel auto-combustion route using sucrose as fuel and study of their structural, magnetic and electrical properties. Ceramics International, 2016, 42, 14475-14489.	2.3	61
27	Stabilization of temperature during magnetic hyperthermia by Ce substituted magnetite nanoparticles. Journal of Magnetism and Magnetic Materials, 2017, 434, 181-186.	1.0	61
28	Correlation between site preference and magnetic properties of Co–Zr doped BaCo x Zr x Fe (12 â^2 x) O 19 prepared under sol–gel and citrate precursor sol–gel conditions. Journal of Alloys and Compounds, 2014, 615, 875-881.	2.8	59
29	Study of magnetic behavior in co-precipitated Ni–Zn ferrite nanoparticles and their potential use for gas sensor applications. Journal of Magnetism and Magnetic Materials, 2020, 502, 166534.	1.0	58
30	Exploring the structural, Mössbauer and dielectric properties of Co2+ incorporated Mg0.5Zn0.5â^'xCoxFe2O4 nanocrystalline ferrite. Journal of Magnetism and Magnetic Materials, 2014, 360, 21-33.	1.0	55
31	Cations distribution and magnetic properties of Co–Zr doped BaCo x Zr x Fe (12â^'2x) O 19 prepared via citrate precursor sol–gel route. Ceramics International, 2014, 40, 16617-16626.	2.3	55
32	Zn _x Fe _{3â^'x} O ₄ (0.01 ≤i>x ≤0.8) nanoparticles for controlled magnetic hyperthermia application. New Journal of Chemistry, 2018, 42, 7144-7153.	1.4	55
33	Structural and electron spin resonance spectroscopic studies of Mn Zn1â^'Fe2O4 (x =â€0.5, 0.6, 0.7) nanoferrites synthesized by sol-gel auto combustion method. Journal of Magnetism and Magnetic Materials, 2018, 466, 60-68.	1.0	53
34	Fe3C nanoparticles for magnetic hyperthermia application. Journal of Magnetism and Magnetic Materials, 2019, 481, 251-256.	1.0	51
35	Enhanced dielectric, magnetic and optical properties of Cr-doped BiFeO3 multiferroic nanoparticles synthesized by sol-gel route. Results in Physics, 2019, 13, 102299.	2.0	50
36	Effect of Fuel on the Synthesis, Structural, and Magnetic Properties of M-Type Hexagonal SrFe12O19 Nanoparticles. Journal of Superconductivity and Novel Magnetism, 2015, 28, 1589-1599.	0.8	49

#	Article	IF	CITATIONS
37	Investigation of structural and magnetic properties of co-precipitated Mn–Ni ferrite nanoparticles in the presence of α-Fe2O3 phase. Journal of Magnetism and Magnetic Materials, 2015, 392, 101-106.	1.0	49

The distinctive compositional evolution of glauconite in the Cretaceous Ukra Hill Member (Kutch) Tj ETQq000 rgBI $_{.5}$ Overlock 10 Tf 50

39	Magnetic interactions and dielectric dispersion in Mg substituted M-type Sr-Cu hexaferrite nanoparticles prepared using one step solvent free synthesis technique. Ceramics International, 2018, 44, 4426-4435.	2.3	49
40	Modulation of physico-chemical, magnetic, microwave and electromagnetic properties of nanocrystalline strontium hexaferrite by Co-Zr doping synthesized using citrate precursor sol-gel method. Ceramics International, 2017, 43, 590-598.	2.3	48
41	Investigation of cation distribution and magnetocrystalline anisotropy of Ni x Cu 0.1 Zn 0.9â^'x Fe 2 O 4 nanoferrites: Role of constant mole percent of Cu 2+ dopant in place of Zn 2+. Ceramics International, 2017, 43, 7984-7991.	2.3	47
42	Catalytic properties of dispersed iron oxides Fe2O3/MO2 (MÂ=ÂZr, Ce, Ti and Si) for sulfuric acid decomposition reaction: Role of support. International Journal of Hydrogen Energy, 2018, 43, 37-52.	3.8	47
43	Manganese ferrite prepared using reverse micelle process: Structural and magnetic properties characterization. Journal of Alloys and Compounds, 2015, 642, 70-77.	2.8	46
44	Distinctive compositional characteristics and evolutionary trend of Precambrian glaucony: Example from Bhalukona Formation, Chhattisgarh basin, India. Precambrian Research, 2015, 271, 33-48.	1.2	45
45	Structural and magnetic properties of glass-ceramics containing silver and iron oxide. Materials Chemistry and Physics, 2012, 133, 144-150.	2.0	44
46	Synthesis of nanosize and sintered Mn0.3Ni0.3Zn0.4Fe2O4 ferrite and their structural and dielectric studies. Journal of Alloys and Compounds, 2013, 555, 225-231.	2.8	44
47	Structural and magnetic properties of spin chain compoundsCa3Co2â^'xFexO6. Physical Review B, 2006, 74, .	1.1	43
48	Structural, optical, elastic and magnetic properties of Ce and Dy doped cobalt ferrites. Journal of Alloys and Compounds, 2020, 834, 155089.	2.8	43
49	Structural, thermal and magnetic studies of MgxZn1â^'xFe2O4 nanoferrites: Study of exchange interactions on magnetic anisotropy. Ceramics International, 2016, 42, 19179-19186.	2.3	42
50	Facile single phase synthesis of Sr, Co co-doped BiFeO3 nanoparticles for boosting photocatalytic and magnetic properties. Applied Surface Science, 2019, 493, 593-604.	3.1	42
51	Preparation and studies on surface modifications of calcium-silico-phosphate ferrimagnetic glass-ceramics in simulated body fluid. Materials Science and Engineering C, 2009, 29, 2226-2233.	3.8	41
52	Electrical resistivity and Mössbauer studies of Cr substituted Co nano ferrites. Journal of Alloys and Compounds, 2017, 694, 366-374.	2.8	41
53	Gamma radiation roused lattice contraction effects investigated by Mössbauer spectroscopy in nanoparticle Mn–Zn ferrite. Radiation Physics and Chemistry, 2014, 102, 147-152.	1.4	39
54	Modified surface and bulk properties of Fe-substituted lanthanum titanates enhances catalytic activity for CO+N2O reaction. Journal of Molecular Catalysis A, 2011, 335, 158-168.	4.8	36

#	Article	IF	CITATIONS
55	Influence of Co4+-Ca2+ substitution on structural, microstructure, magnetic, electrical and impedance characteristics of M-type barium–strontium hexagonal ferrites. Ceramics International, 2020, 46, 24816-24830.	2.3	36
56	Î ³ -Fe2O3 nanoflowers as efficient magnetic hyperthermia and photothermal agent. Applied Surface Science, 2021, 560, 150025.	3.1	36
57	High temperature dielectric studies of indium-substituted NiCuZn nanoferrites. Journal of Physics and Chemistry of Solids, 2018, 112, 29-36.	1.9	34
58	Multiferroic properties of microwave sintered BaTiO3–SrFe12O19 composites. Physica B: Condensed Matter, 2014, 448, 323-326.	1.3	33
59	Catalytic and redox properties of nano-sized La0.8Sr0.2Mn1â^xFexO3â~î^ mixed oxides synthesized by different routes. Journal of Molecular Catalysis A, 2006, 246, 128-135.	4.8	32
60	Study of structural, electrical and magnetic properties of Cr doped Ni–Mg ferrite nanoparticle. Journal of Alloys and Compounds, 2014, 602, 150-156.	2.8	32
61	Structural and magnetic characterization of Zr-substituted magnetite (Zr x Fe 3â^'x O 4 , 0≤ â‰≇). Journal of Magnetism and Magnetic Materials, 2016, 401, 559-566.	1.0	32
62	Crystal structure and magnetic properties of Bi0.8A0.2FeO3 (A = La, Ca, Sr, Ba) multiferroics using neutron diffraction and Mossbauer spectroscopy. AIP Advances, 2014, 4, .	0.6	31
63	Magnetic and dielectric properties of Zn substituted cobalt oxide nanoparticles. Ceramics International, 2019, 45, 16512-16520.	2.3	31
64	Synthesis of exchange coupled nanoflowers for efficient magnetic hyperthermia. Journal of Magnetism and Magnetic Materials, 2019, 484, 437-444.	1.0	31
65	Influence of samarium doping on structural, elastic, magnetic, dielectric, and electrical properties of nanocrystalline cobalt ferrite. Applied Physics A: Materials Science and Processing, 2021, 127, 1.	1.1	31
66	Structural and magnetic properties of nanocrystalline equi-atomic spinel high-entropy oxide (AlCoFeMnNi)3O4 synthesised by microwave assisted co-precipitation technique. Journal of Alloys and Compounds, 2021, 878, 160269.	2.8	31
67	Investigation of structural, magnetic and dielectric properties of gallium substituted Z-type Sr3Co2-Ga Fe24O41 hexaferrites for microwave absorbers. Journal of Alloys and Compounds, 2020, 822, 153470.	2.8	30
68	Effect of heating temperature on structural, magnetic, and dielectric properties of Magnesium ferrites prepared in the presence of Solanum Lycopersicum fruit extract. Journal of Materials Science: Materials in Electronics, 2020, 31, 18445-18463.	1.1	30
69	Nano-aggregates of hexacyanoferrate (II)-loaded magnetite for removal of cesium from radioactive wastes. Journal of Magnetism and Magnetic Materials, 2003, 267, 335-340.	1.0	29
70	Enabling the Electrochemical Activity in Sodium Iron Metaphosphate [NaFe(PO ₃) ₃] Sodium Battery Insertion Material: Structural and Electrochemical Insights. Inorganic Chemistry, 2017, 56, 5918-5929.	1.9	29
71	Design and development of Ga-substituted Z-type hexaferrites for microwave absorber applications: Mössbauer, static and dynamic properties. Ceramics International, 2021, 47, 1145-1162.	2.3	29
72	Physical and chemical properties of nanoscale magnetite-based solvent extractant. Journal of Magnetism and Magnetic Materials, 2005, 293, 8-14.	1.0	28

#	Article	IF	CITATIONS
73	Spin reorientation behavior in YMn1â^'xMxO3 (M=Ti, Fe, Ga; x=0, 0.1). Journal of Magnetism and Magnetic Materials, 2013, 348, 120-127.	1.0	28
74	Core–Shell Prussian Blue Analogue Molecular Magnet Mn _{1.5} [Cr(CN) ₆]· <i>m</i> H ₂ O@Ni _{1.5} [Cr(CN) _{6for Hydrogen Storage. ACS Applied Materials & Interfaces, 2014, 6, 17579-17588.}	ub>∦A∲oxi>n	2
75	Structural and magnetic investigations: Study of magnetocrystalline anisotropy and magnetic behavior of 0.1% Cu2+ substituted Ni–Zn ferrite nanoparticles. Ceramics International, 2018, 44, 1193-1200.	2.3	28
76	Studies of structural, magnetic and dielectric properties of X-type Barium Zinc hexaferrite Ba2Zn2Fe28O46 powder prepared by combustion treatment method using ginger root extract as a green reducing agent. Journal of Alloys and Compounds, 2020, 842, 155120.	2.8	28
77	Study of structural and magnetic properties of (Co–Cu)Fe2O4/PANI composites. Materials Chemistry and Physics, 2013, 141, 406-415.	2.0	27
78	Controlled synthesis and enhanced tunnelling magnetoresistance in oriented Fe ₃ O ₄ nanorod assemblies. Journal Physics D: Applied Physics, 2018, 51, 085002.	1.3	27
79	Investigation on structural, hysteresis, Mössbauer properties and electrical parameters of lightly Erbium substituted X-type Ba2Co2Er Fe28-O46 hexaferrites. Ceramics International, 2020, 46, 8209-8226.	2.3	27
80	Evaluation of structural and dielectric properties of Mn2+-substituted Zn-spinel ferrite nanoparticles for gas sensor applications. Sensors and Actuators B: Chemical, 2020, 316, 128127.	4.0	27
81	Large tunneling magnetoresistance in octahedral Fe3O4 nanoparticles. AIP Advances, 2016, 6, .	0.6	26
82	Study of structural and magnetic properties of Li–Ni nanoferrites synthesized by citrate-gel auto combustion method. Ceramics International, 2016, 42, 2941-2950.	2.3	26
83	Quantification of site disorder and its role on spin polarization in the nearly half-metallic Heusler alloy NiFeMnSn. Physical Review B, 2016, 94, .	1.1	25
84	Biocompatible suspension of nanosized γâ€Fe2O3 synthesized by novel methods. Journal of Applied Physics, 2005, 97, 10Q903.	1.1	24
85	Investigation of structural, dielectric, magnetic and antibacterial activity of Cu–Cd–Ni–FeO4 nanoparticles. Journal of Magnetism and Magnetic Materials, 2013, 341, 148-157.	1.0	24
86	Evidence for the Existence of Oxygen Clustering and Understanding of Structural Disorder in Prussian Blue Analogues Molecular Magnet M _{1.5} [Cr(CN) ₆]· <i>z</i> H ₂ O (M = Fe and Co): Reverse Monte Carlo Simulation and Neutron Diffraction Study. Journal of Physical Chemistry C, 2013, 117, 2676-2687.	1.5	24
87	Immobilization of crystalline Fe2O3 nanoparticles over SiO2 for creating an active and stable catalyst: A demand for high temperature sulfuric acid decomposition. Applied Catalysis B: Environmental, 2021, 283, 119610.	10.8	24
88	Nanoscale-driven structural changes and associated superparamagnetism in magnetically diluted Ni–Zn ferrites. Materials Chemistry Frontiers, 2018, 2, 300-312.	3.2	23
89	Enhanced electrical, magnetic and optical behaviour of Cr doped Bi0.98Ho0.02FeO3 nanoparticles. Journal of Alloys and Compounds, 2019, 796, 229-236.	2.8	23
90	Glauconite authigenesis during the onset of the Paleocene-Eocene Thermal Maximum: A case study from the Khuiala Formation in Jaisalmer Basin, India. Palaeogeography, Palaeoclimatology, Palaeoecology, 2021, 571, 110388.	1.0	23

#	Article	IF	CITATIONS
91	Phase separations inLa0.7â^'xDyxCa0.3Mn(Fe)O3. Physical Review B, 2005, 71, .	1.1	22
92	Magnetic proximity effect in ferrimagnetic–ferromagnetic core–shell Prussian blue analogues molecular magnet. Chemical Physics Letters, 2016, 651, 155-160.	1.2	22
93	Structural investigations on Mo, Cs and Ba ions-loaded iron phosphate glass for nuclear waste storage application. Journal of Alloys and Compounds, 2021, 850, 156715.	2.8	22
94	Influence of Ni2+ substitution on the structural, dielectric and magnetic properties of Cu–Cd ferrite nanoparticles. Journal of Alloys and Compounds, 2013, 573, 198-204.	2.8	21
95	Quaternary ammonium bearing hyper-crosslinked polymer encapsulation on Fe ₃ O ₄ nanoparticles. RSC Advances, 2016, 6, 21317-21325.	1.7	21
96	Study of Higher Discharge Capacity, Phase Transition, and Relative Structural Stability in Li ₂ FeSiO ₄ Cathode upon Lithium Extraction Using an Experimental and Theoretical Approach and Full Cell Prototype Study. ACS Applied Energy Materials, 2019, 2, 6584-6598.	2.5	21
97	Study of structural, vibrational, elastic and magnetic properties of uniaxial anisotropic Ni-Zn nanoferrites in the context of cation distribution and magnetocrystalline anisotropy. Journal of Alloys and Compounds, 2021, 873, 159748.	2.8	21
98	Transport and magnetic properties of Fe doped CaMnO3. Journal of Applied Physics, 2012, 112, .	1.1	20
99	A facile gel-combustion route for fine particle synthesis of spinel ferrichromite: X-ray and Mössbauer study on effect of Mg and Ni content. Materials Research Bulletin, 2014, 50, 172-177.	2.7	20
100	Superparamagnetic behavior of indium substituted NiCuZn nano ferrites. Journal of Magnetism and Magnetic Materials, 2015, 381, 416-421.	1.0	20
101	Anisotropy and domain state dependent enhancement of single domain ferrimagnetism in cobalt substituted Ni–Zn ferrites. New Journal of Chemistry, 2016, 40, 9275-9284.	1.4	20
102	Structural phases and Maxwell–Wagner relaxation in magnetically soft-ZnFe2O4 and hard-Sr2Cu2Fe12O22 nanocomposites. Ceramics International, 2016, 42, 2289-2298.	2.3	20
103	Optimization of lithium content in LiFePO ₄ for superior electrochemical performance: the role of impurities. RSC Advances, 2018, 8, 1140-1147.	1.7	20
104	High Mg-glauconite in the Campanian Duwi Formation of Abu Tartur Plateau, Egypt and its implications. Journal of African Earth Sciences, 2019, 156, 12-25.	0.9	20
105	TiO ₂ -Doped Ni _{0.4} Cu _{0.3} Zn _{0.3} Fe ₂ O ₄ Nanoparticles for Enhanced Structural and Magnetic Properties. ACS Omega, 2021, 6, 17931-17940.	1.6	20
106	Synthesis of CoFe Prussian blue analogue/poly vinylidene fluoride nanocomposite material with improved thermal stability and ferroelectric properties. New Journal of Chemistry, 2018, 42, 4567-4578.	1.4	19
107	Stability of ferroelectric phases and magnetoelectric response in multiferroic (1-x)Bi(Ni1/2Ti1/2)O3-PbTiO3/xNi0.6Zn0.4Fe2O4 particulate composites. Ceramics International, 2019, 45, 23013-23021.	2.3	19
108	Multiferroic properties and Mössbauer Study of M-type hexaferrite PbFe12O19 synthesized by the high energy ball milling. Materials Characterization, 2021, 177, 111168.	1.9	18

#	Article	IF	CITATIONS
109	BaTiO3/(Co0.8Ni0.1Mn0.1Fe1.9Ce0.1O4) composites: Analysis of the effect of Co0.8Ni0.1Mn0.1Fe1.9Ce0.1O4 doping at different concentrations on the structural, morphological, optical, magnetic, and magnetoelectric coupling properties of BaTiO3. Ceramics International, 2022, 48, 30499-30509.	2.3	18
110	Rietveld refinement and FTIR spectroscopic studies of Ni2+-substituted Zn-ferrite nanoparticles. Applied Physics A: Materials Science and Processing, 2019, 125, 1.	1.1	17
111	Effect of cobalt-doping on dielectric, magnetic and optical properties of BiFeO3 nanocrystals synthesized by sol – gel technique. Solid State Sciences, 2020, 102, 106168.	1.5	17
112	Hydrothermally synthesized oxalate and phenanthroline based ferrimagnetic one-dimensional spin chain molecular magnets [{Fe(Δ)Fe(Λ)}1â^'x{Cr(Δ)Cr(Λ)}x(ox)2(phen)2]n (x = 0, 0.1 and 0.5) with giant coercivity of 3.2 Tesla. Journal of Materials Chemistry C, 2013, 1, 6637.	2.7	16
113	Magnetic and dielectric behavior in YMn1â^'xFexO3 (x â‰ 8 €‰0.5). Journal of Applied Physics, 2014, 115, 21	13911.	16
114	Effects of sintering temperature on microstructure, initial permeability and electric behaviour of Ni-Mn-Zn ferrites. Materials Chemistry and Physics, 2022, 275, 125250.	2.0	16
115	Investigation of magnetic properties for Hf4+ substituted CeO2 nanoparticles for spintronic applications. Journal of Materials Science: Materials in Electronics, 2018, 29, 10614-10623.	1.1	15
116	Effect of non-stoichiometry in lead hexaferrites on magnetic and dielectric properties. Materials Chemistry and Physics, 2018, 220, 137-148.	2.0	15
117	Magnetic field regulated, controlled hyperthermia with Li Fe3-O4 (0.06 ≤ ≤0.3) nanoparticles. Ceramics International, 2019, 45, 12028-12034.	2.3	15
118	Magnetic nanocomposites of Fe3C or Ni-substituted (Fe3C/Fe3O4) with carbon for degradation of methylene orange and p-nitrophenol. Journal of Cleaner Production, 2021, 309, 127372.	4.6	15
119	Investigation of structural and magnetic properties of La doped Co–Mn ferrite nanoparticles in the presence of α-Fe2O3 phase. Solid State Communications, 2022, 342, 114629.	0.9	15
120	Influence of Au addition on magnetic properties of iron oxide in a silica–phosphate glass matrix. Journal of Magnetism and Magnetic Materials, 2013, 345, 24-28.	1.0	14
121	xmins:mml="http://www.w3.org/1998/Math/Math/Math/MathWL" display="inline"> <mml:msub><mml:mrow /><mml:mn>3</mml:mn></mml:mrow </mml:msub> Co <mml:math xmlns:mml="http://www.w3.org/1998/Math/MathML" display="inline"><mml:msub><mml:mrow /><mml:mn>2</mml:mn></mml:mrow </mml:msub>O<mml:math< td=""><td>1.1</td><td>14</td></mml:math<></mml:math 	1.1	14
122	Amins.mine "http://www.wo.org/1999/MathMathMethMethMethMethMethMethMethMethMethMe	2.8	14
123	Effect of Copper Substitution on the Structural, Magnetic, and Dielectric Properties of M-Type Lead Hexaferrite. Journal of Electronic Materials, 2020, 49, 6024-6039.	1.0	14
124	Physical and in-vitro evaluation of ϵ-Fe3N@Fe3O4 nanoparticles for bioapplications. Ceramics International, 2020, 46, 10952-10962.	2.3	14
125	Influence of Mn Substitution on Mössbauer and Magnetic Properties of Ni-Zn Ferrite Nanoparticles. Journal of Superconductivity and Novel Magnetism, 2017, 30, 3241-3246.	0.8	13
126	Influence of addition of Al3+ on the structural and solid state properties of nanosized Ni–Zn ferrites synthesized using malic acid as a novel fuel. Journal of Alloys and Compounds, 2020, 842, 155855.	2.8	13

#	Article	IF	CITATIONS
127	Tailoring magnetic and dielectric properties of SrFe12O19/NiFe2O4 ferrite nanocomposites synthesized in presence of Calotropis gigantea (crown) flower extract. Journal of Alloys and Compounds, 2022, 900, 163415.	2.8	13
128	Magnetic and electric properties of nanoparticles of Ni-substituted ferrites synthesized using a microwave refluxing process. International Journal of Materials Research, 2013, 104, 680-685.	0.1	12
129	Assembled diglycolamide for f-element ions sequestration at high acidity. Reactive and Functional Polymers, 2014, 74, 52-57.	2.0	12
130	One-Dimensional Single-Chain Molecular Magnet with a Cross-Linked π–π Coordination Network [{Co ^{II} (Δ)Co ^{II} (Λ)}(ox) ₂ (phen) ₂] _{<i>n</i>} . Journal of Physical Chemistry C, 2014, 118, 1864-1872.	1.5	12
131	Revealing structural distortion and dielectric relaxation in Ga1â^'Sc FeO3 (0≤â‰0.3). Journal of Magnetism and Magnetic Materials, 2016, 417, 165-174.	1.0	12
132	Synthesis and structural characterization of Co _x Fe _{3â^'x} C (0 ≤i>x ≤0.3) magnetic nanoparticles for biomedical applications. New Journal of Chemistry, 2019, 43, 3536-3544.	1.4	12
133	Structural and electrochemical investigation of binary Na2Fe1-xZnxP2O7 (0 ≤ ≤) pyrophosphate cathodes for sodium-ion batteries. Journal of Solid State Chemistry, 2019, 277, 329-336.	1.4	12
134	Structural and electrochemical performance studies for nanocomposites of carbon with Fe3C or Mn-Substituted (Fe3C/Fe3O4) as anodes for Li-batteries. Applied Surface Science, 2020, 533, 147474.	3.1	12
135	Evaluation of Structural, Micro-structural, Vibrational and Elastic Properties of Ni–Cu–Zn Nanoferrites: Role of Dopant Cu2+ at Constant 0.1 mol% in Ni–Zn Spinel Structure. Journal of Inorganic and Organometallic Polymers and Materials, 2021, 31, 1336-1346.	1.9	12
136	Preparation of cellulose-based biocompatible suspension of nano-sized /spl gamma/-Al/sub x/Fe/sub 2-x/O/sub 3/. IEEE Transactions on Magnetics, 2005, 41, 4099-4101.	1.2	11
137	Hydrogen absorption characteristics and Mössbauer spectroscopic study of Ti0.67Nb0.33â^'xFex (x=0.00,) Tj l	ETQ <u>9</u> 110.	784314 rgB
138	Preparation, Electrical and Magnetic Properties of Poly(m-phenylenediamine)/ZnFe2O4 Nanocomposites. Journal of Superconductivity and Novel Magnetism, 2018, 31, 497-504.	0.8	11
139	Sustainable preparation of sunlight active α-Fe ₂ O ₃ nanoparticles using iron containing ionic liquids for photocatalytic applications. RSC Advances, 2019, 9, 41803-41810.	1.7	11
140	Electrical and magnetic properties of poly(m-phenylenediamine)/NiFe2O4 nanocomposites. Journal of Materials Science: Materials in Electronics, 2017, 28, 15754-15761.	1.1	10
141	Synthesis, Spectral and Biological Studies of Complexes with Bidentate Azodye Ligand Derived from Resorcinol and 1-Amino-2-Naphthol-4-Sulphonic Acid. Oriental Journal of Chemistry, 2018, 34, 45-54.	0.1	10
142	Synthesis, characterization & biological studies of Mn(II), Fe(III) and Co(II) complexes of (Z)-1, 5-dimethyl-4-(2-(2-oxopropylidene) hydrazinyl)-2-phenyl-1H-pyrazol-3(2H)-one. Journal of Molecular Structure, 2020, 1201, 127110.	1.8	10
143	Structural and in-vitro assessment of Zn Fe3â^'C (0Ââ‰ÂxÂâ‰Â1) nanoparticles as magnetic biomaterials. Applied Surface Science, 2020, 509, 144891.	3.1	10
144	Magnetic, electrical and gas sensing properties of poly(o-phenylenediamine)/MnCoFe2O4 nanocomposites. Applied Physics A: Materials Science and Processing, 2020, 126, 1.	1.1	10

#	Article	IF	CITATIONS
145	Effect on the structure and stability of iron phosphate glass with Sb and Te-ion loading for nuclear waste storage application. Journal of Non-Crystalline Solids, 2021, 570, 121016.	1.5	10
146	Critical composition of for high CMR. Journal of Magnetism and Magnetic Materials, 2007, 311, 594-604.	1.0	9
147	Mn-substituted cerium oxide nanostructures and their magnetic properties. Materials Research Bulletin, 2018, 104, 65-71.	2.7	9
148	Quantification of charge carriers participating antiferromagnetic to weak ferromagnetic phase transition in Na doped LaFeO3 nano multiferroics. Journal of Applied Physics, 2018, 124, 084102.	1.1	9
149	Surface engineered Tb and Co co-doped BiFeO3 nanoparticles for enhanced photocatalytic and magnetic properties. Journal of Materials Science: Materials in Electronics, 2021, 32, 7956-7972.	1.1	9
150	Shielding performance of Mn Ni0.8–Zn0.2Fe2O4 (0.1≤â‰ 9 .7) for electromagnetic interference (EMI) in X-band frequency. Ceramics International, 2022, 48, 9987-9997.	2.3	9
151	Synthesis, structural characterization and biological studies of Ni(II), Cu(II) and Fe(III) complexes of hydrazone derived from 2-(2-(2,2-dimethyl-4,6-dioxo-1,3-dioxan-5-ylidene)hydrazinyl)benzoic acid. Inorganica Chimica Acta, 2022, 536, 120919.	1.2	9
152	Mössbauer study of KMnFeF6. Solid State Communications, 2000, 116, 575-580.	0.9	8
153	Structural development and magnetic phenomenon in Zn–Cr–Fe multi oxide nano-crystals. Ceramics International, 2014, 40, 8357-8368.	2.3	8
154	Room temperature ferroelectricity in one-dimensional single chain molecular magnets [{M(Δ)M(ŀ)}(ox)2(phen)2]n (M = Fe and Mn). Applied Physics Letters, 2017, 110, 102901.	1.5	8
155	Mössbauer Study and Curie Temperature Configuration on Sintering Nano-Ni-Zn Ferrite Powder. Journal of Superconductivity and Novel Magnetism, 2019, 32, 2141-2147.	0.8	8
156	Spontaneous exchange bias in high energy ball milled MnBi alloys. Journal of Magnetism and Magnetic Materials, 2022, 557, 169478.	1.0	8
157	Magnetic Carrier for Radionuclide Removal from Aqueous Wastes: Parameters Investigated in the Development of Nanoscale Magnetite Based Carbamoyl Methyl Phosphine Oxide. Separation Science and Technology, 2006, 41, 925-942.	1.3	7
158	Ferromagnetic Bismuth-Substituted CeO2 Nanostructures and Prevalence of Antiferromagnetic Clusters. Journal of Superconductivity and Novel Magnetism, 2020, 33, 3941-3947.	0.8	7
159	MnFe2O4 nano-flower: A prospective material for bimodal hyperthermia. Journal of Alloys and Compounds, 2022, 899, 163192.	2.8	7
160	Green synthesis based X-type Ba–Zn Hexaferrites: Their structural, Hysteresis, Mӧssbauer, dielectric and electrical properties. Materials Chemistry and Physics, 2022, 282, 125914.	2.0	7
161	Structural and Mossbauer spectroscopic studies of heat-treated Ni[sub x]Zn[sub 1â^'x]Fe[sub 2]O[sub 4] ferrite nanoparticles. , 2013, , .		6
162	Fe–Ni solid solutions in nano-size dimensions: Effect of hydrogen annealing. Materials Research Bulletin, 2016, 74, 447-451.	2.7	6

#	Article	IF	CITATIONS
163	Zinc oxide functionalized human hair: A potential water decontaminating agent. Journal of Colloid and Interface Science, 2016, 462, 307-314.	5.0	6
164	Investigation of Resistivity, Magnetic Susceptibility and Dielectric Properties of Nanocrystalline Ni-Mn-Zn Ferrites. Journal of Superconductivity and Novel Magnetism, 2017, 30, 1287-1292.	0.8	6
165	Zr-substituted cobalt oxide nanoparticles: structural, magnetic and electrical properties. Journal of Materials Science: Materials in Electronics, 2019, 30, 20088-20098.	1.1	6
166	Formation of non-alloyed Ti/Al/Ni/Au low-resistance ohmic contacts on reactively ion-etched n-type GaN by surface treatment for GaN light-emitting diodes applications. Applied Physics A: Materials Science and Processing, 2019, 125, 1.	1.1	6
167	Effect of crystallite size on the phase transition behavior of heterosite FePO ₄ . Physical Chemistry Chemical Physics, 2020, 22, 15478-15487.	1.3	6
168	Paleoenvironmental Conditions during the Paleocene–Eocene Transition Imprinted within the Glauconitic Giral Member of the Barmer Basin, India. Minerals (Basel, Switzerland), 2022, 12, 56.	0.8	6
169	Plasma polymerized functional supermagnetic Fe3O4 nanostructured templates for laccase immobilization: A robust catalytic system for bio-inspired dye degradation. Environmental Science and Pollution Research, 2022, 29, 82524-82540.	2.7	6
170	Phase separation in La0.67Ca0.33Mn0.9Fe0.1O3: a Mössbauer study. Journal of Physics Condensed Matter, 2004, 16, 1665-1678.	0.7	5
171	Mol̀^ssbauer spectroscopic study of heat-treated (Ni0.5Zn0.5)Fe2O4 nanoparticles. AIP Conference Proceedings, 2012, , .	0.3	5
172	Synthesis and spectral studies of metal complexes of a Schiff base derived from (2-amino-5-chlorophenyl)phenyl methanone. Spectrochimica Acta - Part A: Molecular and Biomolecular Spectroscopy, 2015, 151, 598-604.	2.0	5
173	Structural, Conductivity, and Dielectric Properties of Co0.5Mg0.5La0.1Fe1.9O4 Ferrite Nanoparticles. Journal of Superconductivity and Novel Magnetism, 2016, 29, 2813-2819.	0.8	5
174	Effect of precursors on the structural, magnetic, dielectric, microwave and electromagnetic properties of Co–Zr doped nanocrystalline strontium hexaferrites synthesized via sol–gel method. SN Applied Sciences, 2019, 1, 1.	1.5	5
175	Physical and in vitro evaluation of ultra-fine cohenite particles for the prospective magnetic hyperthermia application. Journal of Materials Science: Materials in Electronics, 2020, 31, 10772-10782.	1.1	5
176	Characterization study and recovery of copper from low grade copper ore through hydrometallurgical route. Advanced Powder Technology, 2022, 33, 103382.	2.0	5
177	Aqueous spray-drying synthesis of alluaudite Na2+2xFe2â^'x(SO4)3 sodium insertion material: studies of electrochemical activity, thermodynamic stability, and humidity-induced phase transition. Journal of Solid State Electrochemistry, 2022, 26, 1941-1950.	1.2	5
178	Spin glass ordering of Zn0.75Co0.25Fe0.5Cr1.5O4 cubic spinel. Solid State Communications, 2003, 126, 535-540.	0.9	4
179	Effect of Co-Zr doping in the M-Type barium hexaferrite BaCoxZrxFe(12-2x)O19: A Mol^ss. AlP Conference Proceedings, 2012, , .	0.3	4

180 $M \tilde{A} \P$ ssbauer spectroscopic study of iron-chelate trammels. , 2014, , .

#	Article	lF	CITATIONS
181	Synthesis of Fe-Si-B-Mn-based nanocrystalline magnetic alloys with large coercivity by high energy ball milling. Bulletin of Materials Science, 2014, 37, 815-821.	0.8	4
182	Controlling structural distortion in the geometrically frustrated layered cobaltate YBaCo4O7+Îby Fe substitution and its role on magnetic correlations. Materials Research Express, 2015, 2, 026102.	0.8	4
183	Structural and magnetic properties of Prussian blue analogue molecular magnet Fe1.5[Cr(CN)6]·mH2O. AlP Conference Proceedings, 2016, , .	0.3	4
184	SEM, magnetization and Mössbauer spectroscopic characterization of Fe-U sequestration. AIP Conference Proceedings, 2017, , .	0.3	4
185	Characterization of PAH matrix with monazite stream containing uranium, gadolinium and iron. AIP Conference Proceedings, 2016, , .	0.3	3
186	The effect of Mn on the structural and magnetic behaviour of Fe–6Si–8B alloy produced by high energy ball Milling. Transactions of the Indian Institute of Metals, 2017, 70, 1431-1436.	0.7	3
187	DPASV analytical technique for ppb level uranium analysis. AIP Conference Proceedings, 2018, , .	0.3	3
188	Study of Magnetic and Electrical Properties of Poly(o-phenylenediamine)/Manganese Substituted ZnFe2O4 Nanocomposites. Journal of Inorganic and Organometallic Polymers and Materials, 2021, 31, 3441-3459.	1.9	3
189	Magnetic, Dielectric and Ethanol Gas Sensing Properties of Poly(o-phenylenediamine)/(MnNi)Fe2O4 Nanocomposites and Quantum Chemical Calculations of (MnNi)Fe2O4. Journal of Inorganic and Organometallic Polymers and Materials, 2022, 32, 2173-2191.	1.9	3
190	Mössbauer study of superconducting Bi2Sr2Ca2Cu3(1â^'x)Fe3xO10. Solid State Communications, 1999, 109, 311-316.	0.9	2
191	Spectroscopic studies on Fe(II) and Fe(III) complexes of 5-aryl azo substituted IH-pyrimidine-2,4-dione. AIP Conference Proceedings, 2013, , .	0.3	2
192	Synthesis and characterization of Fe (III) complex of an azo dye derived from (2-amino-5-chlorophenyl) phenyl methanone. AIP Conference Proceedings, 2013, , .	0.3	2
193	Sintering effect on structural and magnetic properties of Ni[sub 0.6]Zn[sub 0.4]Fe[sub 2]O[sub 4] ferrite. , 2013, , .		2
194	Synthesis of Superparamagnetic Nanoparticle Ni0.50Zn0.50Fe2O4 Using Wet Chemical Method. Journal of Superconductivity and Novel Magnetism, 2014, 27, 2829-2833.	0.8	2
195	Superparamagnetic behavior of heat treated Mg0.5Zn0.5Fe2O4 ferrite nanoparticles studied by MA¶ssbauer spectroscopy. AIP Conference Proceedings, 2016, , .	0.3	2
196	Impact of annealing temperature on structural, optical, and Mössbauer properties of nanocrystalline NiFe2O4. Journal of Materials Science: Materials in Electronics, 2021, 32, 27232-27242.	1.1	2
197	Preparation of silica xerogel beads embedded with Fe2O3 nanoparticles and their characterization. Journal of Nanoparticle Research, 2021, 23, 1.	0.8	2
198	Size dependent electronic structure of LiFePO ₄ probed using X-ray absorption and Mössbauer spectroscopy. Physical Chemistry Chemical Physics, 2022, 24, 9695-9706.	1.3	2

#	Article	IF	CITATIONS
199	Neutron diffraction study of quasi-one-dimensional spin-chain compounds Ca3Co2–x Fe x O6. Pramana - Journal of Physics, 2008, 71, 923-927.	0.9	1
200	Spectroscopic studies on two mono nuclear iron (III) complexes derived from a schiff base and an azodye. , 2014, , .		1
201	Synthesis and spectral study of new azo dye and its iron complexes derived from 2-naphthol and 2-amino-3-hydroxypyridine. AIP Conference Proceedings, 2014, , .	0.3	1
202	Fe2-xCoxMnSi (x = 0, 1 and 2) Heusler alloys: Structural, magnetic and atomic site disorder properties. AIP Conference Proceedings, 2015, , .	0.3	1
203	Effect of heat treatment on structural and Mössbauer spectroscopic properties of coprecipitated Mn0.5Ni0.5Fe2O4 ferrite nanoparticles. AlP Conference Proceedings, 2015, , .	0.3	1
204	Structural and magnetic properties of Cr doped BiFeO3 multiferroic nanoparticles. AIP Conference Proceedings, 2017, , .	0.3	1
205	Effect of Cu2+ substitution on the magnetic properties of co-precipitated Ni-Cu-Zn ferrite nanoparticles. AIP Conference Proceedings, 2017, , .	0.3	1
206	Characterization of Nano-Particle Co1â^'x Zn x Fe2O4 Synthesized Using Alove Vera Gel. Journal of Superconductivity and Novel Magnetism, 2017, 30, 395-399.	0.8	1
207	Pre-concentration technique for reduction in "Analytical instrument requirement and analysis― AIP Conference Proceedings, 2018, , .	0.3	1
208	Structural and magnetic properties of ordered inverse spinel Li Fe5O8. Journal of Alloys and Compounds, 2021, 865, 158849.	2.8	1
209	Studies on the uranium speciation in zinc iron phosphate (ZnIP) glass using Mössbauer and EXAFS spectroscopic investigations. Ceramics International, 2021, 47, 18323-18329.	2.3	1
210	Process hybridization for nuclear effluent treatment. AIP Conference Proceedings, 2020, , .	0.3	1
211	Characterization and Mol̀^ssbauer Study of Ni[sub 0.45]Zn[sub 0.55]Fe[sub 2]O[sub 4] Nanoparticles Prepared by Novel Precursor Method. , 2011, , .		0
212	Synthesis of nanoparticles Ni0.55Zn0.45Fe2O4 by novel precursor method showing enhanced resistivity. , 2012, , .		0
213	Structural, dielectric and Mossbauer studies of sol-gel synthesized nano Ni-Cu-Zn ferrites. , 2013, , .		0
214	Structural and magnetic properties of BaCo[sub x]Zr[sub x]Fe[sub (12-2x)]O[sub 19] prepared by citrate precursor sol-gel route. , 2013, , .		0
215	Effect of microwave sintering on structural and magnetic properties of SrFe <inf>12</inf> O <inf>19</inf> nanopowders. , 2013, , .		Ο
216	Structural and MoÌ^ssbauer spectroscopic study of cubic phase hydrogen storage alloys Ti[sub 2]Nb[sub 1â^'x]Fe[sub x]. , 2013, , .		0

#	Article	IF	CITATIONS
217	Effect of Co2+ substitution in Mg0.5Zn0.5â^'xCoxFe2O4 ferrite nanoparticles: Study of structural, dielectric and magnetic properties. , 2014, , .		0
218	Structural and MÃ \P ssbauer spectroscopic study of Fe-Ni alloy nanoparticles. , 2014, , .		0
219	Mössbauer spectroscopic study of cobalt hexacyanoferrate nanoparticles: Effect of hydrogenation. AIP Conference Proceedings, 2018, , .	0.3	0
220	Structural and Mössbauer analysis of pure and Ce-Dy doped cobalt ferrite nanoparticles. AIP Conference Proceedings, 2018, , .	0.3	0
221	Fine particle effects on the magnetic behaviour of Mn–substituted Zn–ferrite nanoparticles. AlP Conference Proceedings, 2019, , .	0.3	0
222	Characterization and performance of nuclear plant floor washed effluent treated resin. AIP Conference Proceedings, 2019, , .	0.3	0
223	Mineralogical studies of low grade iron ore from Bellary-Hospet region, India. AIP Conference Proceedings, 2019, , .	0.3	0
224	Insight into structural aspects and study of reaction kinetics of model [oxo(salen)iron(IV)] complexes with dipeptides. Polyhedron, 2021, 196, 114952.	1.0	0
225	Physical and in-vitro evaluation of pure and substituted MxCe1-xO2 (M = Co, Fe or Ti and x = 0.05) magnetic nanoparticles. Ceramics International, 2021, 47, 8812-8819.	2.3	0
226	Morphological and chromatographical characterization of RAD-effluent trammelled resin. AIP Conference Proceedings, 2020, , .	0.3	0
227	Effect of synthesis temperature on magnetization and properties of Y-Fe-garnet. AIP Conference Proceedings, 2020, , .	0.3	0
228	Structural and Mössbauer spectroscopic studies of Mn-substituted Cu-ferrite nanoparticles. AIP Conference Proceedings, 2020, , .	0.3	0